Electron Tunneling in Single Crystals of *Pseudomonas aeruginosa* Azurins

Brian R. Crane,† Angel J. Di Bilio, Jay R. Winkler, and Harry B. Gray*

Contribution from the Beckman Institute, California Institute of Technology, Pasadena, California 91125

Received June 28, 2001

Abstract: Rates of reduction of Os(III), Ru(III), and Re(I)* by Cu(I) in His83-modified *Pseudomonas aeruginosa* azurins (M−Cu distance ∼17 Å) have been measured in single crystals, where protein conformation and surface solvation are precisely defined by high-resolution X-ray structure determinations: $1.7(8) \times 10^6$ s^{-1} (298 K), $1.8(8) \times 10^6$ s^{-1} (140 K), [Ru(bpy)$_2$(im)$^{3+}$-]; $3.0(15) \times 10^6$ s^{-1} (298 K), [Ru(tpy)(bpy)$^{3+}$-]; $3.0(15) \times 10^6$ s^{-1} (298 K), [Ru(tpy)(phen)$^{3+}$-]; $9.0(50) \times 10^2$ s^{-1} (298 K), [Os(bpy)$_2$(im)$^{3+}$-]; $4.4(20) \times 10^6$ s^{-1} (298 K), [Re(CO)$_3$(phen)$^{+}$*] (bpy = 2,2′-bipyridine; im = imidazole; tpy = 2,2′:6′,2″-terpyridine; phen = 1,10-phenanthroline). The time constants for electron tunneling in crystals are roughly the same as those measured in solution, indicating very similar protein structures in the two states. High-resolution structures of the oxidized (1.5 Å) and reduced (1.4 Å) states of Ru(II)(tpy)(phen)(His83)Az establish that very small changes in copper coordination accompany reduction but reveal a shorter axial interaction between copper and the Gly45 peptide carbonyl oxygen [2.6 Å for Cu(II)] than had been recognized previously. Although Ru(bpy)$_2$(im)(His83)Az is less solvated in the crystal, the reorganization energy for Cu(I) → Ru(III) electron transfer falls in the range (0.6−0.8 eV) determined experimentally for the reaction in solution. Our work suggests that outer-sphere protein reorganization is the dominant activation component required for electron tunneling.

Electron transfer (ET) between metal redox centers in proteins often occurs over distances greater than 10 Å and at rates unparalleled by other types of reactions.[1−16] The dependence of these distant ET rates on the structure of the intervening medium has been elucidated in studies of Ru-modified iron and copper proteins.[2−4,17] Notably, work on selectively engineered derivatives of *Pseudomonas aeruginosa* azurin[18,19] has led to experimentally validated timetables for electron tunneling through polypeptide structures.[1−4]

Our analyses of tunneling rate relationships have involved a key assumption, namely, that Ru-modified protein structures are not very different in crystals and aqueous solutions. We are currently testing this assumption by investigating ET kinetics of sensitizer-modified azurins in single crystals, where protein and solvent structures are defined by X-ray diffraction analyses. The copper complex in the blue protein is embedded in an 8-stranded antiparallel β barrel, with one extra-barrel helix inserted between β4 and β5 (numbered from the N-terminus).[20] The copper is trigonally coordinated by donor atoms from the side chains of Cys112, His46, and His117 in a hydrophobic cluster at one end of the β barrel; and the Met121 thioether and Gly45 peptide carbonyl are weak axial ligands.

The azurin copper center is readily reduced and reoxidized in solution, owing to its low reorganization energy ($\lambda \sim 0.7$ eV).[21−23] The relative contributions of inner-sphere and outer-sphere components to this reorganization are not known with certainty, but reasonable estimates are available.[24−28] Consistent with a low inner-sphere reorganization energy, the structures of oxidized [Cu(II)] and reduced [Cu(I)] proteins exhibit only small changes in copper coordination.[23]

* Address correspondence to this author: (e-mail) hbgray@caltech.edu.
† Present address: Department of Chemistry and Chemical Biology, Cornell University, Ithaca, NY 14853.

(1) Tezcan, F. A.; Crane, B. R.; Winkler, J. R.; Gray, H. B. *Proc. Natl. Acad. Sci. U.S.A.* **2001**, *98*, 5002−5006.
(2) Winkler, J. R. *Curr. Opin. Chem. Biol.* **2000**, *4*, 192−198.
(3) Winkler, J. R.; Di Bilio, A. J.; Farrow, N. A.; Richards, J. H.; Gray, H. B. *Pure Appl. Chem.* **1999**, *71*, 1753−1764.
(4) Gray, H. B.; Winkler, J. R. *Annu. Rev. Biochem.* **1996**, *65*, 537−561.
(5) Mei, H. K.; Wang, K. F.; Peffer, N.; Weatherly, G.; Cohen, D. S.; Miller, M.; Pielak, G.; Durham, B.; Millett, F. *Biochemistry* **1999**, *38*, 6846−6854.
(6) Farver, O.; Pecht, I. *JBIC* **1997**, *2*, 387−392.
(7) Dick, L. A.; Malfant, I.; Kuila, D.; Nebolsky, S.; Nocek, J. M.; Hoffman, B. M.; Ratner, M. A. *J. Am. Chem. Soc.* **1998**, *120*, 11401−11407.
(8) Ramirez, B. E.; Malmström, B. G.; Winkler, J. R.; Gray, H. B. *Proc. Natl. Acad. Sci. U.S.A.* **1995**, *92*, 11949−11951.
(9) Onuchic, J. N.; Beratan, D. N.; Winkler, J. R.; Gray, H. B. *Annu. Rev. Biophys. Biomol. Struct.* **1992**, *21*, 349−377.
(10) Beratan, D. N.; Skourtis, S. S. *Curr. Opin. Chem. Biol.* **1998**, *2*, 235−243.
(11) Daizadeh, I.; Gehlen, J. N.; Stuchebrukhov, A. A. *J. Phys. Chem.* **1997**, *106*, 5658−5666.
(12) Page, C. C.; Moser, C. C.; Chen, X.; Dutton, P. L. *Nature* **1999**, *402*, 47−52.
(13) Williams, R. J. P. *JBIC* **1997**, *2*, 373−377.
(14) McLendon, G.; Hake, R. *Chem. Rev.* **1992**, *92*, 481−490.
(15) Nocek, J. M.; Zhou, J. S.; De Forest, S.; Priyadarshy, S.; Beratan, D. N.; Onuchic, J. N.; Hoffman, B. M. *Chem. Rev.* **1996**, *96*, 2459−2489.
(16) Davidson, V. L. *Acc. Chem. Res.* **2000**, *33*, 87−93.
(17) Babini, E.; Bertini, I.; Borsari, M.; Capozzi, F.; Luchinat, C.; Zhang, X. Y.; Moura, G. L. C.; Kurnikov, I. V.; Beratan, D. N.; Ponce, A.; Di Bilio, A. J.; Winkler, J. R.; Gray, H. B. *J. Am. Chem. Soc.* **2000**, *122*, 4532−4533.
(18) Langen, R.; Chang, I.-J.; Germanas, J. P.; Richards, J. H.; Winkler, J. R.; Gray, H. B. *Science* **1995**, *268*, 1733−1735.
(19) Langen, R.; Colon, J. L.; Casimiro, D. R.; Karpishin, T. B.; Winkler, J. R.; Gray, H. B. *JBIC* **1996**, *1*, 221−225.
(20) Adman, E. T. *Adv. Protein Chem.* **1991**, *42*, 145−197.
(21) Di Bilio, A. J.; Hill, M. G.; Bonander, N.; Karlsson, B. G.; Villahermosa, R. M.; Malmström, B. G.; Winkler, J. R.; Gray, H. B. *J. Am. Chem. Soc.* **1997**, *119*, 9921−9922.
(22) Skov, L. K.; Pascher, T.; Winkler, J. R.; Gray, H. B. *J. Am. Chem. Soc.* **1998**, *120*, 1102−1103.
(23) Gray, H. B.; Malmström, B. G.; Williams, R. J. P. *JBIC* **2000**, *5*, 551−559.

10.1021/ja0115870 CCC: $20.00
Published on Web 11/01/2001

Table 1. X-ray Data Collection, Refinement and Metal Occupancy Statistics for Metal-Modified Azurin Structures

sensitizer oxidation state	Ru(II)(tpy)(phen)-Cu(II)	Ru(II)(tpy)(phen)-Cu(I)	Ru(II)(bpy)$_2$(im)-Cu(II)	Ru(II)(tpy)(bpy)-Cu(II)	Re(I)(CO)$_3$(phen)-Cu(II)	Os(II)(bpy)$_2$(im)-Cu(II)
resolution (Å)	30.0−1.5	30.0−1.4	20.0−1.6	20.0−1.7	20.0−1.6	30.0−1.8
X-ray wavelength[a] (Å)	1.03	1.03	1.08	1.08	1.08	1.54
completeness	98.9	98.4	92.1	98.0	98.7	97.4
$\langle I/\sigma I\rangle$[b]	32	30	34	26	19	36
R_{sym}[c] (%)	3.8	4.5	5.0	5.9	8.0	7.2
R[d] (%)	21.7	22.6	24.9	26.9	22.7	22.2
free R[e] (%)	22.1	23.3	27.4	27.7	24.8	26.0
rms bond[f] (Å)	0.01	0.01	0.03	0.01	0.01	0.01
rms angel[f] (deg)	1.3	1.4	1.5	1.3	1.3	1.4
PDB code	1JZF	1JZG	1JZE	1JZH	1JZI	1JZJ

[a] Diffraction data were collected at SSRL BL-71 (1.08 (Å), SSRL BL-91 (1.03 Å), and a rotating anode X-ray source (1.54 Å). [b] Intensity signal-to-noise ratio. [c] $R_{sym} = \sum\sum_j|I_j - \langle I\rangle|\sum\sum_j I_j$. [d] $R = \sum||F_{obs}| - |F_{calc}||/\sum|F_{obs}|$ for all reflections (no σ cutoff). [e] Free R calculated against 8% of the reflections removed at random. [f] Root-mean-square deviations from bond and angle restraints.

We have developed methods to trigger and monitor ET between metalloprotein active centers and inorganic sensitizers in protein single crystals. Employing these techniques, we have examined both driving force and temperature effects on Cu(I) → Ru(III), Os(III), and Re(I)* ET rates in single crystals of His83-modified azurins, where the surrounding medium is significantly different from that in aqueous solution, yet the conformational integrity of the protein is maintained. Our results show conclusively that a folded polypeptide can facilitate electron tunneling between distant donors and acceptors in crystals.

Experimental Section

Metal-Modified Azurins. *P. aeruginosa* azurin was expressed in *E. coli* and purified as described previously.[29] Ru(II)(bpy)$_2$(im)(His83)-Az (bpy = 2,2′-bipyridine; im = imidazole; Az = azurin) and Re(I)-(CO)$_3$(phen)(His83)AzM^{2+} (phen = 1,10-phenanthroline; M = Cu, Zn) were prepared by standard procedures.[30,31] Ru(II)(tpy)(L)(His83)Az (tpy = 2,2′:6′,2″-terpyridine; L = bpy or phen) was obtained following the general procedure employed in the preparation of Ru-modified plastocyanin.[32] Os(II)(bpy)$_2$(im)(His83)Az was prepared as follows: Os(II)(bpy)$_2$(CO$_3$)[33] was incubated with 2.0 mM azurin in 250 mM $NaHCO_3$ (pH 8.3) for 4−7 days at 37 °C. After removing unreacted osmium by gel-filtration, Os(III)(bpy)$_2$(OH)(His83)Az was purified on a Cu-chelating column and then with cation exchange chromatography.[30,31] After exchanging Os(III)(bpy)$_2$(OH)(His83)Az into 500 mM imidazole (pH 8.5), the solution was titrated under anaerobic conditions with aqueous dithionite until it turned a bright red color indicative of Os(II)(bpy)$_2$(H$_2$O)(His83)Az (λ_{max} = 512 nm). Over a period of 12 h the solution changed color from red to orange as imidazole substitution occurred to give Os(II)(bpy)$_2$(im)(His83)Az (λ_{max} = 485 nm). Os(II)-(bpy)$_2$(im)(His83)Az was then exchanged into 40 mM imidazole (pH 7.2), 2 mM NaCl for crystallization.

Electrochemistry of Os(II)(bpy)$_2$(im)(His83)Az. The potentials of Os(II)(bpy)$_2$(im)(His83)Az were determined by cyclic voltammetry in 0.1 M sodium phosphate buffer (pH 7.0) by using an edge-plane graphite (EPG) working electrode, platinum auxiliary electrode, and a Ag/AgCl reference electrode. Prior to use the EPG electrode was polished with 0.3 mm alumina, sonicated, and rinsed with distilled water. The Os(III/II) potential was determined to be 522 mV (NHE) and the Cu(II/I) couple to be 322 mV (NHE), the latter virtually the same as that of the native protein.[34]

Crystal Growth and Manipulation. Metal-modified azurin crystals were grown by vapor diffusion from solutions of 20−30 mg/mL of protein in 40 mM imidazole, 2 mM NaCl (pH 7.2) which was mixed 50/50 by volume with reservoirs consisting of 100 mM imidazole (pH 6.0−8.0), 100 mM $LiNO_3$, 6.25 mM $CuCl_2$, and 25−38% poly(ethylene glycol) (PEG, MW 4000−8000). RuAz and ReAz crystals grew within a pH range of 6.0−8.0. The complex Cu(II)(im)$_4$(OH$_2$)$_2$ mediated crystal contacts in all cases. Diffraction quality OsAz crystals only grew at pH 6.0 anaerobically. Although a solution of Os(II)(bpy)$_2$(im)(His83)-Az was stable in air for days at 4 °C, crystals grown aerobically only contained Os(III). Crystals for ET experiments were grown from degassed solutions in an anerobic chamber. For flash-quench ET experiments with $[Ru(NH_3)_6]^{3+}$, crystals were reduced with 1 mM ascorbate, washed in stabilizing PEG solutions, and then transferred to PEG solutions containing 10 mM $[Ru(NH_3)_6]^{3+}$ at least 2 h before measuring kinetics.

Crystal Structure Determination. Diffraction data for RuAz and ReAz crystal forms were collected at the Stanford Synchrotron Radiation Laboratory on beam line 7-1 with a Mar image plate or beam line 9-2 with a ADSC quantum IV CCD; data for OsAz crystals were collected on an R-Axis IV image plate mounted on a Rigaku X-ray generator (Table 1). Crystals were flash-cooled at 100 K. Diffraction data were processed with DENZO.[35] Molecular replacement was carried out with AMoRe[36] or EPMR[37] by using a probe derived from a 2.3 Å resolution structure of Ru(II)(bpy)$_2$(im)(His83)Az (PDB code: 1BEX).[30] Rigid-body, simulated annealing, positional, and thermal factor maximum-likelihood refinement was performed with CNS,[38] amidst rounds of manual rebuilding, sensitizer incorporation, and water placement with XFIT.[39] All residues have favored backbone dihedral angles. Both Δ and Λ isomers were modeled for Ru(II)(bpy)$_2$(im)(His83) and Os(II)-(bpy)$_2$(im)(His83). Stereochemical restraints were removed from the copper ligand bonds in later stages of refinement. Multiple copper and ligand starting coordinates were chosen to test convergence of

(24) Randall, D. W.; Gamelin, D. R.; Lacroix, L. B.; Solomon, E. I. *JBIC* **2000**, *5*, 16−29.
(25) Larsson, S. *JBIC* **2000**, *5*, 560−564.
(26) Ryde, U.; Olsson, M. H. M.; Roos, B. O.; de Kerpel, J. O. A.; Pierloot, K. *JBIC* **2000**, *5*, 565−574.
(27) Ryde, U.; Olsson, M. H. M. *Int. J. Quantum Chem.* **2001**, *81*, 335−347.
(28) Sigfridsson, E.; Olsson, M. H. M.; Ryde, U. *J. Phys. Chem. B* **2001**, in press.
(29) Piccioli, M.; Luchinat, C.; Mizoguchi, T. J.; Ramirez, B. R.; Gray, H. B.; Richards, J. R. *Inorg. Chem.* **1995**, *34*, 737−742.
(30) Faham, S.; Day, M. W.; Connick, W. B.; Crane, B. R.; Di Bilio, A. J.; Schaefer, W. P.; Rees, D. R.; Gray, H. B. *Acta Crystallogr.* **1999**, *D55*, 379−385.
(31) Di Bilio, A. J.; Crane, B. R.; Wehbi, W. A.; Kiser, C.; Abu-Omar, M. M.; Carlos, R. M.; Richards, J. H.; Winkler, J. R.; Gray, H. B. *J. Am. Chem. Soc.* **2001**, *123*, 3181−3182.
(32) Di Bilio, A. J.; Dennison, C.; Gray, H. B.; Sykes, A. G.; Ramirez, B. E.; Winkler, J. R. *J. Am. Chem. Soc.* **1998**, *120*, 7551−7556.
(33) Kober, E. M.; Caspar, J. V.; Sullivan, B. P.; Meyer, T. J. *Inorg. Chem.* **1988**, *27*, 4587−4598.
(34) Pascher, T.; Karlsson, B. G.; Nordling, M.; Malmström, B. G.; Vänngård, T. *Eur. J. Biochem.* **1993**, *212*, 289−296.
(35) Otwinowski, Z.; Minor, M. *Methods Enzymol.* **1997**, *276*, 307−326.
(36) Navaza, J. *Acta Crystallogr.* **1994**, *A50*, 157−163.
(37) Kissinger, C. R.; Gehlhaar, D. K.; Fogel, D. B. *Acta Crystallogr.* **1999**, *D55*, 484−491.
(38) Brunger, A.; Adams, P. D.; Clore, G. M.; Delano, W. L.; Gros, P.; Grosse-Kunstleve, R. W.; Jiang, J. S.; Kuszewski, J.; Nilges, M.; Pannu, N. S.; Read, R. J.; Rice, L. M.; Simonson, T.; Warren, G. L. *Acta Crystallogr.* **1998**, *D54*, 905−921.
(39) McRee, D. E. *J. Mol. Graphics* **1992**, *10*, 44−46.

coordination geometry for the high-resolution oxidized and reduced Ru(II)(tpy)(phen)(His83)Az structures.

Structures of Oxidized and Reduced Ru(II)(tpy)(phen)(His83)-Az. Diffraction data were collected at 100 K on oxidized Ru(II)(tpy)-(phen)(His83)Az on SSRL beam-line 9-2 with 12.00 keV radiation. The X-ray energy was then tuned to 7.14 keV and the crystal was irradiated (~15 min) until the K-edge X-ray absorption spectra of the crystal (measured by fluorescence on BL-9-2) showed a shoulder at ~8984 eV in the K-edge spectra, which is diagnostic for Cu(I) azurin.[40,41] Appearance of the ~8984 eV shoulder correlated with a change in the color of the irradiated region from green to orange under polarized light. A second data set was then collected at 12.00 keV on the reduced crystal. X-ray absorption spectroscopy confirmed that the protein in the crystal was still oxidized after the first data set had been obtained.

Steady-State and Time-Resolved Single-Crystal Optical Spectroscopy. A specialized microspectrophotometer was constructed to measure steady-state and time-resolved spectra in single protein crystals. For steady-state spectra, light was directed through the crystal from a 75 W Xe-arc lamp using fiber optic cables. Sets of focusing and collecting microscope objectives produced a 20 μm diameter spot size at the sample. Collected light from the crystal was dispersed by a 600 lines/mm grating onto a 1024 element CCD array (PC-1000 spectrometer, World Precision Instruments). Crystals were dried and mounted in sealed glass capillaries with flat faces. Polarized spectra were recorded by inserting a thin polarizer in the beam path. For time-resolved spectra, crystals were excited with a 100−500 μJ 5−20 ns laser pulse generated either from an XeCl excimer-pumped dye laser or Nd:YAG-pumped OPO and delivered along the probe path to a ~100 μm diameter spot at the sample. Probe light was generated either with a 10 mW HeNe laser (632.8 nm), a 5 μs Xe-flash lamp, or a 75 W Xe CW lamp, depending on the sample. For pulsed light experiments, laser excitation was timed to probe light emission. This amounted to triggering the XeCl excimer or the Nd:YAG Q-switch with a photodiode sensing probe light. Probe light was dispersed with a double 0.1 m monochromator, directed onto a 9-stage Hamamatsu PMT, amplified with a 100 MHz current-sensitive amplifier (gain of 7 mV/μA), and digitized with a Tektronix RTD 710A 200 MS/s digitizer. Timing and data acquisition were controlled with LABVIEW running on a PC. For low-temperature experiments, crystals were mounted in nylon loops and flash-cooled to 140 K in a stream of cold nitrogen gas. Temperature was monitored with a thermocouple at the sample. Diffraction quality was maintained for crystals subjected to laser pulses of less than 1 mJ.

Results and Discussion

We have determined high-resolution structures of *P. aeruginosa* azurin crystals with the protein labeled at His83 with five different Ru-, Re-, and Os-polypyridyl sensitizers (Figure 1, Table 1). Although the space groups vary among metal-modified azurin crystals, the crystal solvent content remains constant and the protein packing arrangements are very similar in each lattice (Figure 2A, Table 2). There are two molecules in the asymmetric unit in crystals of Os(II)(bpy)$_2$(im)(His83)Az, and one of the two sensitizer environments is different from all others throughout the five crystal forms.

Metal(His83)azurin Crystalline Environments. Despite crystallizing in different unit cells (Table 1), the packing environment of each of the metal-modified azurins involves the same azurin tetramer (Figure 2b). The relative monomer orientations within this dimer of dimers are similar to each other and to that in azurin crystal forms reported previously.[42] Dimers interact across a 2-fold symmetric interface involving a hydrophobic patch surrounding His117.[43,44] However, within this packing, azurin monomers shift position relative to one another so that the interprotein contacts mediating this interface can be different among the crystal forms. Furthermore, the sensitizer−protein contacts influence crystal packing. For example, the larger Ru(II)(tpy)(phen)(His83) complex expands the *I*222 unit cell compared to Ru(II)(tpy)(bpy)(His83)Az and Ru(II)(bpy)$_2$-(im)(His83)Az (Table 2). The C2 unit cell of Re(I)(CO)$_3$(phen)-(His83)Az is pseudo *I*222, with a noncrystallographic 2-fold axis along the *ac* diagonal replacing a crystallographic 2-fold axis in the *I*222 crystal. The trigonal $P3_221$ Os(II)(bpy)$_2$(im)-(His83)Az packing differs from the others, but still maintains the azurin tetramer. Thus, the concentration, solvation, and environment of a given azurin molecule are very similar in all the crystals studied (Table 2). Likewise, in all crystal forms, each sensitizer participates in the same lattice contact (Figure 3A), with the exception of one of the two unique molecules in the OsAz trigonal crystal, where the intermolecular contact is made with the N-terminus of an adjacent molecule. Disorder in the interprotein contact that involves the two N-terminal residues on one molecule and the Os complex on the other may explain the difficulty in growing crystals of OsAz compared to RuAz and ReAz.

As observed for the lower resolution structure of Ru(II)(bpy)$_2$-(im)(His83)Az,[30] the bound sensitizer produces only minor changes in the structure of the folded polypeptide. These changes mainly involve the 73−77 loop, which shifts back roughly 1.2 Å to accommodate the sensitizer (Figure 3A).

Copper Coordination. The Cys-S, Met-S, and His-N to Cu bond distances in Ru(II)(tpy)(phen)(His83)Az are similar to corresponding values for the native protein (Table 3). All of the high-resolution structures of metal-modified azurins (pH 6.5−8.0), however, reveal a surprisingly short 2.6 Å bond distance between Cu(II) and the axial Gly45 carbonyl oxygen. A much longer distance (2.95 Å at pH 5.5 and 9.0) was reported previously;[42] for *Alcaligenes denitrificans* azurin, this distance is 3.1 Å.[45] The 2.6 Å separation between the carbonyl oxygen and copper is the shortest axial ligand interaction found in a high-resolution structure of a blue copper protein.[23,46] It is not likely that the sensitizer perturbs the structure, as labeling at a site distant from 83 (107) produces the same copper coordination geometry.[31] Further, the possibility of Zn(II) contamination in the site was ruled out by sufficiently large A_{628}/A_{280} ratios (0.60) as well as by the absence of multiple metal ion positions in 1.5 Å resolution electron density maps; and there was no evidence of Zn(II) in the crystals by X-ray absorbance spectroscopy. We conclude that the 2.6 Å Cu−O bond distance is a distinctive feature of copper coordination in *P. aeruginosa* azurin (Figure 4).

High-resolution structures of Cu(II) (1.5 Å resolution) and Cu(I) (1.4 Å resolution) azurins show little change in copper ligation (Table 3). The most prominent difference is in the Cu to Gly45 carbonyl oxygen bond length, which increases by 0.08 Å in the Cu(I) structure. Care was taken to ensure that the copper was in the appropriate oxidation state, because azurin crystals will photoreduce in the X-ray beam over time. In fact, we employed X-ray photoreduction to produce the Cu(I) state at

(40) DeBeer, S.; Kiser, C. N.; Mines, G. A.; Richards, J. H.; Gray, H. B.; Solomon, E. I.; Hedman, B.; Hodgson, K. O. *Inorg. Chem.* **1999**, *38*, 433−438.

(41) DeBeer, S.; Wittung-Stafshede, P.; Leckner, J.; Karlsson, G.; Winkler, J. R.; Gray, H. B.; Malmström, B.; Solomon, E. I.; Hedman, B.; Hodgson, K. O. *Inorg. Chim. Acta* **2000**, *297*, 278−282.

(42) Nar, H.; Messerschmidt, A.; Huber, R.; van de Kamp, M.; Canters, G. W. *J. Mol. Biol.* **1991**, *221*, 765−772.

(43) van de Kamp, M.; Floris, R.; Hali, F.; Canters, G. W. *J. Am. Chem. Soc.* **1990**, *112*, 907−908.

(44) van de Kamp, M.; Silvestrini, M. C.; Brunori, M.; Beeumen, J. V.; Hali, F.; Canters, G. W. *Eur. J. Biochem.* **1990**, *194*, 109−118.

(45) Shepard, W. E. B.; Anderson, B. F.; Lewandoski, D. A.; Norris, G. E.; Baker, E. N. *J. Am. Chem. Soc.* **1990**, *112*, 7817−1719.

(46) Messerschmidt, A. *Struct. Bond.* **1998**, *90*, 37−68.

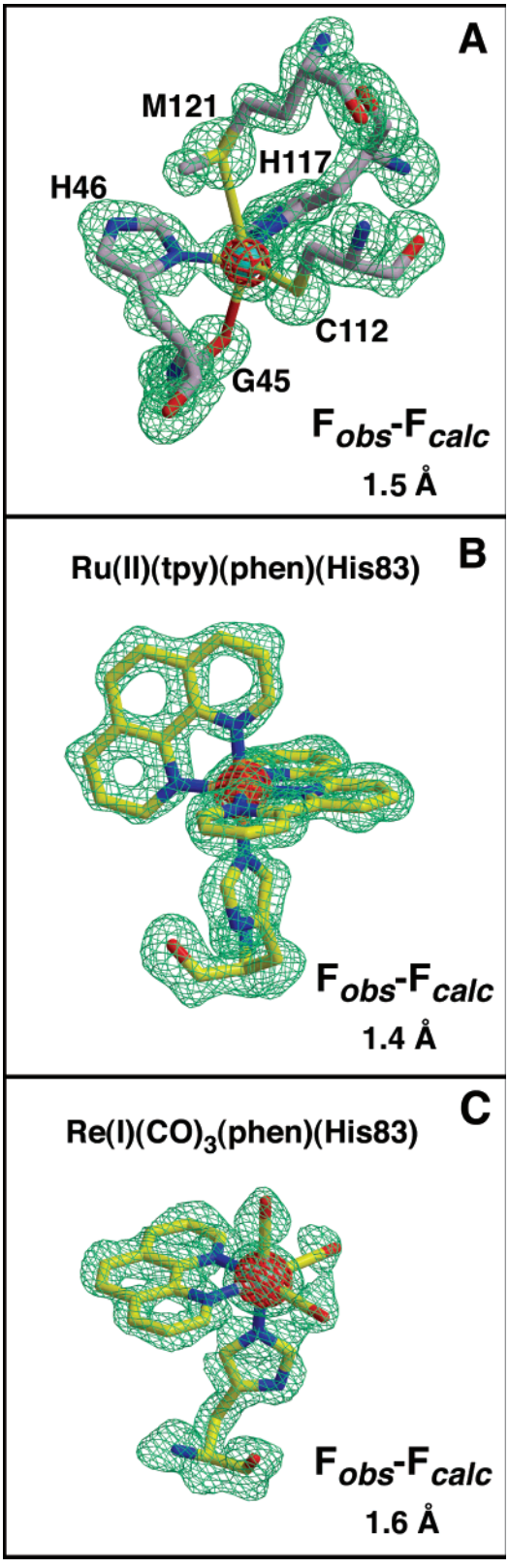

Figure 1. Omit ($F_{obs} - F_{calc}$) electron density: (A) the copper center in Ru(tpy)(phen)AzCu(II) (1.5 Å resolution, contoured at 3.0 σ (green) and 20 σ (red)); (B) the Ru-sensitizer of Ru(II)(tpy)(phen)(His83)-AzCu(I) (1.4 Å resolution contoured at 2.5 σ (green) and 20 σ (red)); and (C) the Re-sensitizer of Re(I)(CO)$_3$(phen)(His83)AzCu(II) (1.6 Å resolution, contoured 2.5 σ (green) and 20 σ (red)). The electron density maps were calculated without displayed regions contributing to F_{calc}.

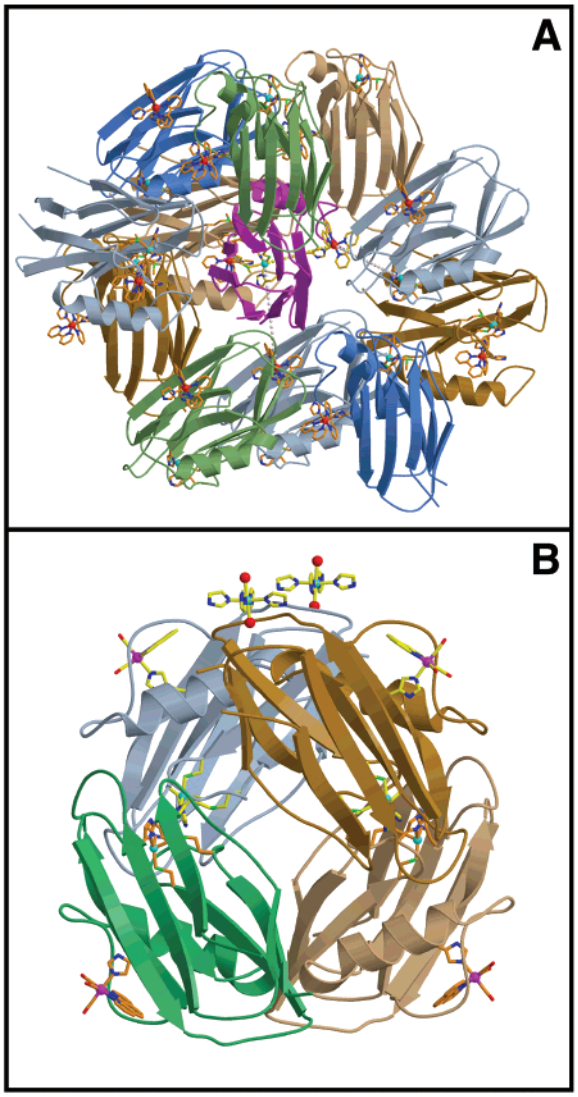

Figure 2. Crystal environment of metal-modified azurins: (A) eleven other molecules (gray, blue, green, and brown ribbons) surround each molecule of Ru(II)(bpy)$_2$(im)(His83)AzCu(II) (purple ribbons) in the crystalline form; Ru(II)(bpy)$_2$(im)(His83) (yellow) and the copper center (cyan copper, yellow ligands) within one molecule are separated across the azurin β-sheet by 17 Å (dotted lines); the next closest Ru−Cu separation (18.5 Å) occurs between molecules, but involves a large through-space jump (the two interprotein paths shown are related by symmetry); (B) the azurin tetramer is present in all crystal forms; Re(I)(CO)$_3$(phen)(His83)Az forms a dimer of dimers by associating via a hydrophobic patch on the surface closest to the copper center; Cu(II)(im)$_4$(H$_2$O)$_2$ complexes (top, yellow) bridge the tetramer to other tetramers (not shown) in the lattice.

the synchrotron beam-line (see Experimental Section). The oxidation state of the crystals before and after the diffraction experiments was monitored by both visible and X-ray absorption spectroscopy.

Reduction also produced no noticeable effect on the structure of the polypeptide or surrounding ordered solvent. In fact, the rms deviation between C$_\alpha$ atoms in the oxidized and reduced structures (0.07 Å) is smaller than values among oxidized structures from different crystals (0.24−0.44 Å). Moreover, difference Fourier maps generated from amplitudes collected from the oxidized and reduced crystals show no significant electron density peaks. Thus, changes in protein dipole orientations that accompany reduction of the copper site are undetected at 1.5 Å resolution.

Table 2. Crystals Formed by Metal-Modified Azurins

	Ru(II)(tpy)(phen)-	Ru(II)(bpy)$_2$(im)-	Ru(II)(tpy)(bpy)-	Re(I) (CO)$_3$(phen)-	Os(II)(bpy)$_2$(im)-
space group	*I*222	*I*222	*I*222	*C*2	$P3_221$
unit cell (Å)^3	52.8 × 61.4 × 76.0	53.4 × 1.8 × 68.8	54.0 × 60.6 × 69.8	94.0 × 51.0 × 62.4 $\beta = 128.1°$	54.9 × 54.9 × 133.8
Z[a]	8	8	8	8	12
solvent content (%)	41	37	37	39	38
protein buried (%)[b]	23	29	30	28, 26[d]	27, 29
sensitizer buried (%)[c]	28	36	39	51, 51[d]	26, 23

[a] Number of azuin molecules per unit cell. [b] Molecular surface area buried in crystal contacts. [c] Sensitizer surface area buried in crystal contacts. [d] For each of two molecules per asymmetric unit. Surface areas calculated with MS (Connolly, M. L. *Science* **1983**, *221*, 709−713); solvent contents calculated from Matthews coefficients (Matthews, B. W. *J. Mol. Biol.* **1968**, *33*, 491−497).

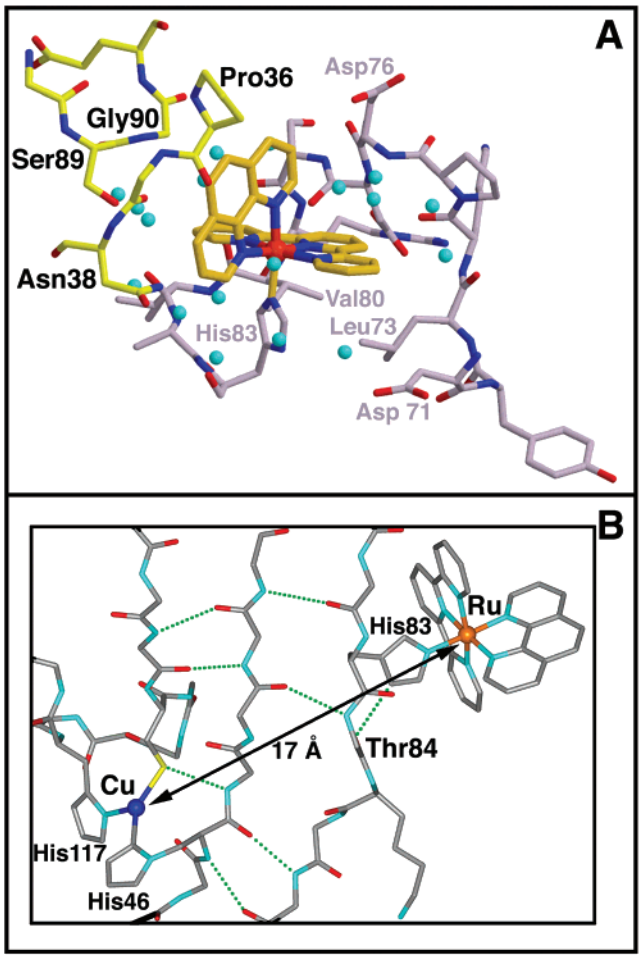

Figure 3. In the dominant crystal environment, the Ru-sensitizer is held within the loop connecting the extra-barrel helix to β5 (residues 73−82) on the molecule that is attached via His83 (A); about one-third of the solvent accessible surface area of the sensitizer is buried by two loops on an adjacent molecule that connect β3 to β4 (residues 36−39) and β5 to β6 (residues 88−91); ET tunneling pathway in azurin (B); a hydrogen-bond network couples Ru(II)(bpy)$_2$(im)(His83) to the blue copper center across the azurin β-sheet.

Single-Crystal Absorption Spectra. Both the RuAz *I*222 and the ReAz pseudo *I*222 crystals are highly dichroic. Complete *a*-axis polarization of the characteristic blue copper absorption (628 nm) accords with the molecular orientation in the crystal, as the S(Cys112)-to-Cu(II) bonds are all aligned along *a* (Figure 5). Thus the blue copper absorption is polarized as predicted for the dipole-allowed S(Cys112)-to-Cu(II) transition;[24,47,48] what is more, there are no significant contributions to the absorption from excitations involving other ligands. Polarization of the 600-nm absorption parallel to CysS−Cu(II) was indicated by spectroscopic measurements on single crystals of plastocyanin, but could not be established unambiguously because of infelicitous molecular alignments relative to crystal axes.[49] Our polarized absorption spectra leave no doubt whatever that the copper is very strongly coupled to the cysteine thiolate through interactions that have been elucidated fully in other spectroscopic investigations[24,47] as well as electronic structure calculations.[24−26,47,48,50,51]

Electron Transfer. Laser excitation of the sensitizers triggers ET to and from the blue copper center (Figure 6), which can be monitored in the crystal by transient absorption spectroscopy. Experiments were carried out in each of the five crystal systems (Figures 7−9). Rate constants for the oxidation of Cu(I) by ground-state Ru(III) and Os(III), as well as excited-state Re(I),[52] are set out in Table 4.

The ET rates in solutions and crystals are very similar for each donor−acceptor pair. *It follows that the potentials and reorganization energies also must be similar in the two cases*[53] *and that the crystal structures of reduced and oxidized azurin are the relevant reactant and product states for solution ET.* The total reorganization energy in the crystal must be roughly equal to $-\Delta G°$ for the Cu(I) → Ru(III) reactions, because Ru(bpy)$_2$(im)(His83)Az ET rates are virtually the same at 298 and 140 K; this places λ in the 0.6−0.8 eV range.[53] The largest difference in ET rate constant between a crystal and solution is for the OsAz complex, where the reaction is roughly 5-fold

(47) Solomon, E. I.; Penfield, K. W.; Gewirth, A. A.; Lowery, M. D.; Shadle, S. E.; Guckert, J. A.; Lacroix, L. B. *Inorg. Chim. Acta* **1996**, *243*, 67−78.

(48) Penfield, K. W.; Gewirth, A. A.; Solomon, E. I. *J. Am. Chem. Soc.* **1985**, *107*, 4519−4529.

(49) Penfield, K. W.; Gay, R. R.; Himmelwright, R. S.; Eickman, N. C.; Norris, V. A.; Freeman, H. C.; Solomon, E. I. *J. Am. Chem. Soc.* **1981**, *103*, 4382−4388.

(50) Larsson, S.; Broo, A.; Sjolin, L. *J. Phys. Chem.* **1995**, *99*, 4860−4865.

(51) Pierloot, K.; de Kerpel, J. O. A.; Ryde, U.; Roos, B. O. *J. Am. Chem. Soc.* **1997**, *119*, 218−226.

(52) Connick, W. B.; Di Bilio, A. J.; Hill, M. G.; Winkler, J. R.; Gray, H. B. *Inorg. Chim. Acta* **1995**, *240*, 169−173.

(53) This conclusion follows from consideration of the semiclassical model for ET in which the rate constant (k) is expressed as a function of driving force ($-\Delta G°$), reorganization energy (λ), electronic coupling strength, and temperature (Marcus, R. A.; Sutin, N. *Biochim. Biophys. Acta* **1985**, *811*, 265−322). If the structures of the proteins are the same in crystal and solution, then only $-\Delta G°$ and λ are likely to be perturbed by crystallization. The total differential of k, then, will be a linear function of the crystallization-induced changes in driving force ($\Delta\Delta G°$) and reorganization energy ($\Delta\lambda$). We solved for $\Delta\Delta G°$ and $\Delta\lambda$ using the solution and crystal ET rates for Ru(bpy)$_2$(im)(His83)Az and Os(bpy)$_2$(im)(His83)Az, for values of the solution reorganization energy λ_{soln} between 0.6 and 0.8 eV.[22] For $\lambda_{soln} > 0.68$ eV, we find $\Delta\Delta G° > 0$ and $\Delta\lambda < 0$; that is, both the driving force and reorganization energy decrease upon crystallization. The $\Delta\Delta G°$ values are inconsistent with ionic-solvation-model predictions that higher Ru(III/II) and Os(III/II) potentials should be found in the crystals because the lattice contact with another protein molecule excludes water from around the sensitizer. More reasonable results are found for $0.58 < \lambda_{soln} < 0.61$ eV. In this region, we find that both $\Delta\Delta G°$ and $\Delta\lambda$ are small and positive (<0.05 eV), supporting the notion that neither driving force nor reorganization energy is substantially modified by crystallization.

Table 3. Copper−Ligand Bond Distances[a] (Å) in Metal-Modified *P. aeruginosa* Azurins

structure	resolution	Cu−N(His46)	Cu−N(His117)	Cu−S(Cys112)	Cu−S(Met121)	Cu−O(Gly45)	ΔCu[d]
Ru(II)(tpy)(phen)AzCu(II)	1.5	2.02	2.08	2.21	3.32	2.60	0.005
Ru(II)(tpy)(phen)AzCu(I)	1.4	2.06	2.12	2.23	3.31	2.68	0.04
AzCu(II) (pH 5.5)[b]	1.9	2.11	2.03	2.25	3.15	2.97	0.10
AzCu(I) (pH 5.5)[b]	1.9	2.14	2.10	2.29	3.25	3.02	0.00
AzCu(II) (pH 9.0)[b]	1.9	2.09	2.04	2.26	3.12	2.95	0.10
AzCu(I) (pH 9.0)[b]	1.9	2.14	2.15	2.27	3.17	3.10	0.00
AzCu(II)[c]	1.8	2.08	2.00	2.15	3.11	3.13	0.12
AzCu(I)[c]	1.8	2.13	2.05	2.26	3.23	3.22	0.14

[a] Averages were taken over crystallographically unique molecules. [b] From ref 46. [c] *A. denitrificans* azurin; ref 45. For tables of blue copper structural parameters see: Libeu, C. A. P.; Kukimoto, M.; Nishiyama, M.; Horinouchi, S.; Adman, E. T. *Biochemistry* **1997**, *36*, 13160−13179 and references 23 and 46. [d] Distance of the Cu from the plane formed by His46ND1, His117ND1, and Cys112SG.

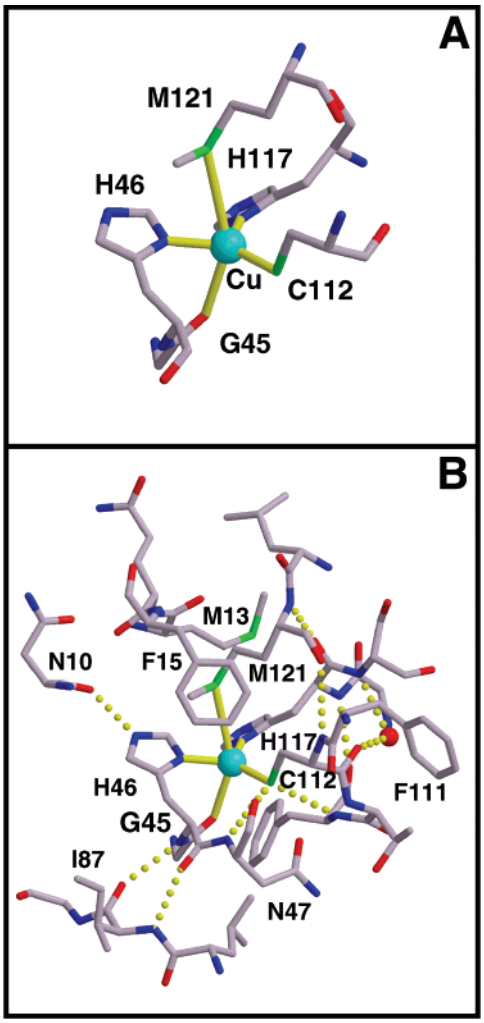

Figure 4. The structure of the copper center in *P. aeruginosa* azurin: (A) trigonal bipyramidal coordination of Cu(II); axial ligands are the Gly45 carbonyl oxygen (Cu−O, 2.6 Å) and the Met121 sulfur (Cu−S, 3.3 Å); (B) hydrophobic residues in the outer sphere encapsulate the active site and protect it from solvent and other potential ligands; all copper ligands except His117 (which is surface exposed) form hydrogen bonds to peripheral residues.

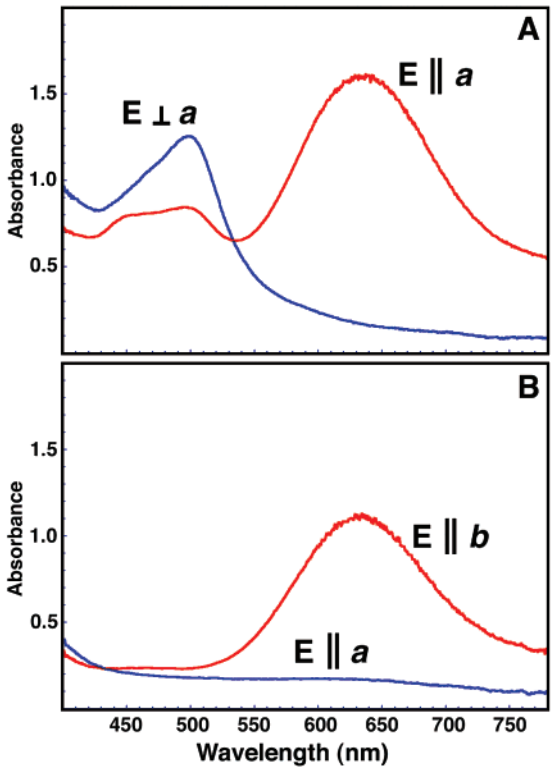

Figure 5. Polarized absorption spectra of single crystals of metal-modified azurins: (A) $Ru(II)(bpy)_2(im)(His83)AzCu(II)$ and (B) $Re(I)(CO)_3(phen)(His83)AzCu(II)$. In RuAz both the blue copper absorption at 628 nm and the $Ru(II)(bpy)_2(im)(His83)$ MLCT band at 450 nm are strongly polarized; the 628-nm absorption is completely polarized along the *a* direction of the *I*222 RuAz crystal and along the *b* axis of the C2 ReAz crystal; the *b* axis in the pseudo *I*222 ReAz C2 crystals corresponds to the *a* axis in the RuAz *I*222 crystals; all of the Cu−S(Cys112) bonds coincide with 2-fold axes along these unit cell directions in each space group.

slower in a crystal.[54] The absence of an inverted effect for the Cu(I) → Re(I)* ET reaction is not unexpected,[55,56] as there are low-lying electronic excited states of Cu(II) that likely are formed as initial products.[24,47]

The hydrogen bond network of the azurin β sheet facilitates electron tunneling between the sensitizer and the copper center (Figure 3b). Calculations indicate that both His83− and Thr84− backbone hydrogen bonds are key elements in the Cu to His83 tunneling tubes;[57−59] and importantly, the imidazole(His83)−

(54) The slower Cu(I) → Os(III) ET observed in OsAz crystals may be a consequence of more acidic crystal-growth conditions (pH 6). Protonation of the His35 residue near the Cu site is accompanied by a backbone peptide bond (Pro36-Gly37) flip[42] and an increase in the Cu(II/I) reduction potential[34] (van de Kamp, M.; Canters, G. W.; Andrew, C. R.; Sandersloehr, J.; Bender, C. J.; Peisach, J. *Eur. J. Biochem.* **1993**, *218*, 229−238). There is evidence in the OsAz X-ray diffraction data that a great many of the protein molecules have adopted the flipped Pro36-Gly37 conformation.

(55) Mines, G. A.; Bjerrum, M. J.; Hill, M. G.; Casimiro, D. R.; Chang, I.-J.; Winkler, J. R.; Gray, H. B. *J. Am. Chem. Soc.* **1996**, *118*, 1961.
(56) Gray, H. B.; Winkler, J. R.; Wiedenfeld, D. *Coord. Chem. Rev.* **2000**, *200−202*, 875−886.
(57) Regan, J. J.; Di Bilio, A. J.; Langen, R.; Skov, L. S.; Winkler, J. R.; Gray, H. B.; Onuchic, J. N. *Chem. Biol.* **1995**, *2*, 489−496.
(58) Regan, J. J.; Di Bilio, A. J.; Winkler, J. R.; Richards, J. H.; Gray, H. B. *Inorg. Chim. Acta* **1998**, *275−276*, 470−480.
(59) Regan, J. J.; Onuchic, J. N. *Adv. Chem. Phys.* **1999**, *107*, 497−533.

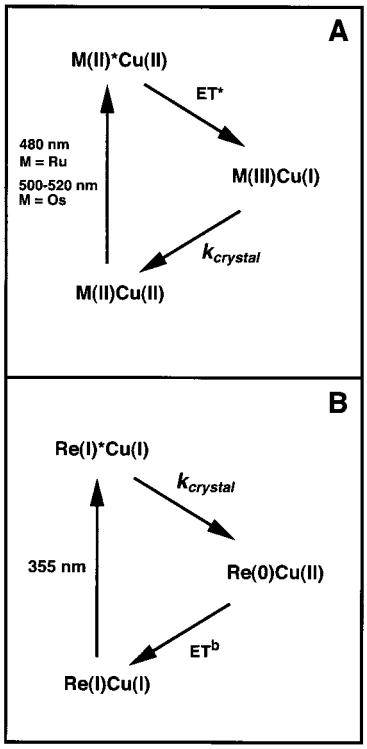

Figure 6. Reaction sequences for metal-modified azurins: (A) photoinduced ET for Ru(II)$(bpy)_2$(im)(His83)AzCu(II), Ru(II)(tpy)(bpy)-(His83)AzCu(II), Ru(II)(tpy)(phen)(His83)AzCu(II), and Os(II)$(bpy)_2$-(im)(His83)Cu(II) [M = Ru: after 480-nm excitation, Ru(II)* reduces Cu(II); $k_{crystal}$ is extracted from the recovery of the Ru(II) MLCT at 430−450 nm and the Cu(II) LMCT at 628 nm as Ru(III) oxidizes Cu(I); M = Os: after 520-nm excitation, Os(II)* reduces Cu(II); $k_{crystal}$ is extracted from the recovery of the Os(II) MLCT at 430−450 nm and the Cu(II) LMCT at 628 nm as Os(III) oxidizes Cu(I)]; (B) photoinduced ET for Re(I)$(CO)_3$(phen)(His83)AzCu(I) [Re(I)* directly oxidizes Cu(I); $k_{crystal}$ was determined from the difference in excited-state lifetimes between Re(I)$(CO)_3$(phen)(His83)AzCu(I) and Re(I)$(CO)_3$(phen)-(His83)AzZn(II); Re(I)* lifetimes were determined at 580 (emission) as well as 450 and 640 nm (transient absorption); 355-nm excitation].

peptide carbonyl bond is maintained in all five structures. Of the two crystallographically unique OsAz molecules, the Os complex with the smaller number of crystal contacts is more disordered than any of the other sensitizers. Thus, conformational fluctuations in solution could alter interactions of the sensitizers with the proteins to which they are attached.

The accessibility of surface sensitizers in the crystal was tested in experiments employing $[Ru(NH_3)_6]^{3+}$ as a quencher. In this reaction, the excited state of Ru(II) reacts with the quencher to form Ru(III), which can then oxidize the reduced protein.[60] An intermediate excited-state lifetime in $[Ru(NH_3)_6]^{3+}$-soaked Cu(I) crystals (100 ns) compared to Cu(I) (200 ns) and Cu(II) (20 ns) crystals indicated some reaction of Ru(II)* with the exogenous quencher.[61] The rate constant extracted from the flash-quench experiment (Figure 7C,D) matches that obtained from direct photoinduction (Table 4) and Cu(I) crystals showed no ET without $[Ru(NH_3)_6]^{3+}$. However, fast rereduction of Cu(II), presumably by $[Ru(NH_3)_6]^{2+}$, suggests that the reductant is near the sensitizer in the crystal. This interaction may be nonspecific, as X-ray diffraction did not reveal a reductant

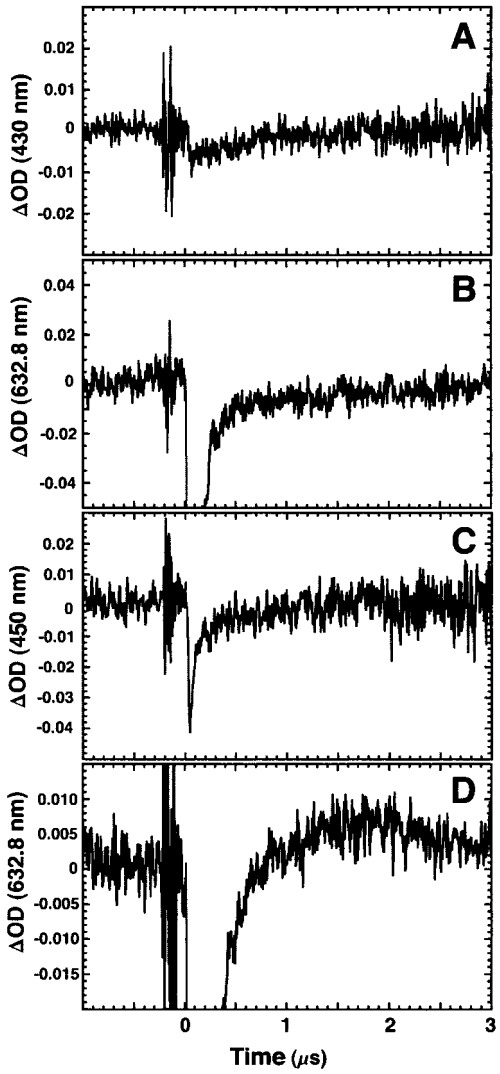

Figure 7. Photoinduced ET for Ru(II)$(bpy)_2$(im)(His83)AzCu(II): trace A shows the recovery of Ru(II) at 430 nm, and an isosbestic point for Ru(II)* (RuAzCu(I) crystals (reduced with ascorbate) exhibit no transient signal at this wavelength); trace B shows emission from Ru(II)* (fast recovery) and the slower recovery of Cu(II) (the slow phase of this biexponential process matches the Ru(II) recovery phase above). Flash-quench ET for Ru(II)$(bpy)_2$(im)(His83)AzCu(I) soaked in $[Ru(NH_3)_6]^{3+}$: trace C contains the initial spike attributable to formation of Ru(II)* and then the slower recovery of Ru(II) from Ru(III); trace D contains the emission from Ru(II)* and then a positive component that represents the formation of Cu(II), and subsequent rereduction by $[Ru(NH_3)_6]^{2+}$. Transient absorption probes: Ru(III), μs-pulsed Xe-flash lamp; Cu(II), HeNe laser (632.8 nm).

binding site. Reactions of sensitizer excited states with exogenous quenchers in crystals could potentially be used to generate reactive intermediates that could be examined by X-ray diffraction methods.

Reorganization Energy. The very modest structural change in copper coordination that accompanies reduction confirms that the azurin inner-sphere reorganization energy is small. Recent analyses of this effect of protein folding on coordination geometry have indicated that the structure is not unfavorable for Cu(II), but is slightly so for Cu(I),[62−65] which prefers a lower coordination number.[23] Indeed, the Cu(II/I) reduction potential

(60) Bjerrum, M. J.; Casimiro, D. R.; Chang, I.-J.; Di Bilio, A. J.; Gray, H. B.; Hill, M. G.; Langen, R.; Mines, G. A.; Skov, L. K.; Winkler, J. R.; Wuttke, D. S. *J. Bioenerg. Biomembr.* **1995**, *27*, 295−302.

(61) Energy transfer as well as electron transfer contributes to Ru(II)* quenching by Cu(II) azurin. Ru(II)* lifetimes were measured by monitoring luminescence at 630 nm.

(62) Leckner, J.; Wittung, P.; Bonander, N.; Karlsson, B. G.; Malmström, B. G. *JBIC* **1997**, *2*, 368−371.

(63) Winkler, J. R.; Wittung-Stafshede, P.; Leckner, J.; Malmström, B. G.; Gray, H. B. *Proc. Natl. Acad. Sci. U.S.A.* **1997**, *94*, 4246−4249.

Table 4. Crystal and Solution ET Rates for Metal-Modified Azurins

modified protein	ET	T (K)	$-\Delta G°$ (eV)[a]	$k_{crystal}$ (s^{-1})[b]	$k_{solution}$ (s^{-1})	Cu−M (Å)[c]
$Ru(bpy)_2(im)$(His83)Az	Cu(I) → Ru(III)	298	0.76	$1.7(8) \times 10^6$	$1.2(1) \times 10^6$	17.05
	Cu(I) → Ru(III)[d]	140	0.76	$1.8(8) \times 10^6$	$3.5(15) \times 10^6$	17.05
	Cu(I) → Ru(III)[e]	298	0.76	$2.0(10) \times 10^6$	$1.2(1) \times 10^6$	17.05
Ru(tpy)(bpy)(His83)Az	Cu(I) → Ru(III)	298	0.76	$3.0(15) \times 10^6$	$2.0(2) \times 10^6$	16.7
Ru(tpy)(phen)(His83)Az	Cu(I) → Ru(III)	298	0.78	$3.0(15) \times 10^6$	$2.7(3) \times 10^6$	16.7
$Os(bpy)_2(im)$(His83)Az	Cu(I) → Os(III)	298	0.20	$9.0(50) \times 10^2$	$4.8(5) \times 10^3$	16.9
$Re(CO)_3(phen)$(His83)Az	Cu(I) → Re(I)*	298	1.17	$4.4(20) \times 10^6$	$1.3(1) \times 10^6$	16.8

[a] Electrochemical potentials taken from ref 21 for RuAz, ref 52 for ReAz, and this work for OsAz. [b] Kinetics were fit to mono-, bi-, or triexponential functions depending on the reaction sequence. [c] Averages taken over unit cell contents. [d] $k_{solution}$ was measured in water/glycerol cryosolvent (65% v/v) at 170 K; ref 22. [e] Flash-quench generation of Ru(III) by reaction of Ru(II)* with $[Ru(NH_3)_6]^{3+}$. Rates are averages from 3 to 5 crystals, with the exception of OsAz, where only one crystal was suitable for both ET and diffraction measurements.

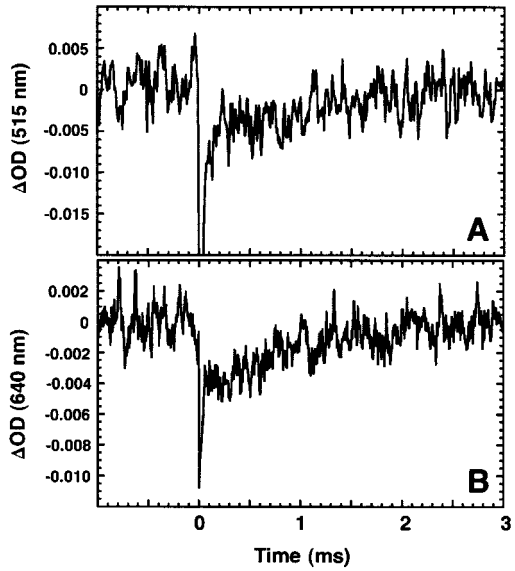

Figure 8. Photoinduced ET for $Os(II)(bpy)_2(im)$(His83)AzCu(II): trace A shows the recovery of Os(II) after initial Cu(II) reduction; trace B shows the recovery of Cu(II). Luminescence from OsAz produces initial spikes in both traces. Crystal transient absorption was probed with a CW Xe-arc lamp.

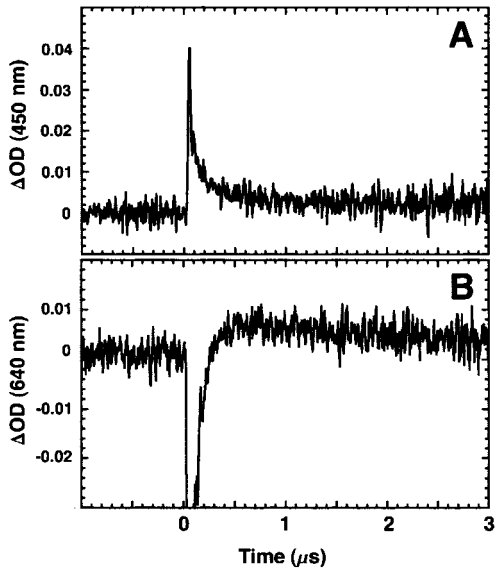

Figure 9. Photoinduced ET for $Re(I)(CO)_3(phen)$(His83)AzCu(I): trace A shows increased absorption attributable to Re(I)*; trace B shows the initial fluorescence of Re(I)* and a positive increase and slower decay that represents formation of Cu(II) by ET and subsequent rereduction by Re(0). ET rates were determined from the difference in Re(I)* lifetimes between ReAzCu(I) and ReAzZn(II). Crystal transient absorption was probed with a μs-pulsed Xe-flash lamp.

increases upon unfolding azurin,[64,65] as ligands to the copper are lost.[41] It follows that the protein gives up more folding free energy to coordinate Cu(I) than Cu(II).[66]

Examination of the azurin structure in the region of the active site reveals that the coordination geometry is constrained by an extensive hydrogen bond network embedded in a cluster of hydrophobic residues (Figure 4b). This outer-sphere "cage" lowers the inner-sphere reorganization energy of the copper center, possibly by as much as 0.5 eV relative to vacuum,[27] thereby allowing rapid electron tunneling at low driving forces.[23] Although our structures show that conformational adjustments to accommodate changes in charge are small and distributed throughout the protein, nevertheless this reorganization of the folded polypeptide itself must be the dominant outer-sphere component of the activation free energy for ET in both solution and crystals. Interestingly, Hoffman and Ratner have reported that ET occurs at near cryogenic temperatures in mixed-metal hemoglobins,[7] in accord with the view[67] that restrained movement of the polypeptide is sufficient for electron tunneling. Calculations including molecular dynamics as employed by Warshel and co-workers[68] in principle could provide a deeper understanding of outer-sphere protein contributions to the overall reorganization energy.

The total protein concentration in prokaryotic cytoplasm (200−300 mg/mL) is only slightly lower than that in azurin crystals (600 mg/mL).[69,70] Macromolecular crowding in cells is thought to have a profound impact on the energetics and dynamics of enzymatic reactions. In a redox process, the extent of polar solvent reorientation could be very sensitive to the precise arrangement of solvent molecules in and around the protein. It is striking, then, that driving forces, reorganization energies, and rates of Cu(I) → Ru(III), Os(III), and Re(I)* ET are virtually unchanged when labeled azurins lose one-third of their solvent accessible surface upon transfer from dilute solutions to crystal lattices with just 40% water. What is more, electron tunneling

(64) Wittung-Stafshede, P.; Hill, M. G.; Gomez, E.; Di Bilio, A. J.; Karlsson, B. G.; Leckner, J.; Winkler, J. R.; Gray, H. B.; Malmström, B. G. *JBIC* **1998**, *3*, 367−370.

(65) Wittung-Stafshede, P.; Gomez, E.; Öhman, A.; Aasa, R.; Villahermosa, R. M.; Leckner, J.; Karlsson, B. G.; Sanders, D.; Fee, J. A.; Winkler, J. R.; Malmström, B. G.; Gray, H. B.; Hill, M. G. *Biochim. Biophys. Acta* **1998**, *1388*, 437−443.

(66) Our high-resolution structures indicate that a Cu−O(carbonyl) interaction must be included in a realistic model of the *P. aeruginosa* azurin Cu site. In fact, only the Cu−O(Gly45) distance changes significantly on reduction (by ~0.08 Å). The 2.6 Å Cu−O axial interaction likely destabilizes Cu(I) and explains the shift toward tetrahedral geometry for Cu(I) coordination (Table 3).

(67) Hoffman, B. M.; Ratner, M. A. *Inorg. Chim. Acta* **1996**, *243*, 233−238.

(68) Muegge, I.; Qi, P. X.; Wand, A. J.; Chu, Z. T.; Warshel, A. *J. Phys. Chem. B* **1997**, *101*, 825−836.

(69) Fulton, A. B. *Cell* **1982**, *30*, 345−347.

(70) Minton, A. P. *Curr. Opinion Biotechnol.* **1997**, *8*, 65−69.

in a $Ru(bpy)_2(im)$(His83)Az crystal is slightly faster at cryogenic temperature than at 298 K (Table 4). Taken together, these observations suggest that bulk water plays a minor role in azurin ET reactions; what little solvent reorganization occurs is likely to involve only the ordered water of hydration.

Biological ET reactions typically involve protein−protein or protein−membrane complexes formed in the crowded confines of cells. Studies in protein crystals could reveal how the exclusion of aqueous solvent from interfacial and exposed surface areas in these complexes affects binding and reactivity. Arguably, protein crystals are the ideal environment for investigations of biological electron tunneling.

Acknowledgment. We thank Mike Machczynski for experimental assistance, Doug Rees and Akif Tezcan for helpful discussions, and SSRL for access to data collection facilities. This research was supported by NIH (DK19038), the Helen Hay Whitney Foundation (fellowship to B.R.C.), and the Arnold and Mabel Beckman Foundation.

Supporting Information Available: Fits to transient absorption kinetics data (PDF). This material is available free of charge via the Internet at http://pubs.acs.org.

JA0115870